JOURNAL OF GEOPHYSICAL RESEARCH VOL. 68, NO. 15 AUGUST 1, 1963

# A Theoretical Photometric Function for the Lunar Surface

BRUCE W. HAPKE

*Center for Radiophysics and Space Research*
*Cornell University, Ithaca, New York*

*Abstract.* A formula describing the observed photometric properties of the lunar surface is derived theoretically. Functions for both the differential and integral brightness are obtained. The model surface on which the derivation is based consists of a semi-infinite, porous layer of randomly placed obscuring objects suspended in depth in such a way that the interstices separating them are interconnected. A layer of fine, loosely compacted dust is in the category of surfaces described by this model, but volcanic foam is not. The shape of the photometric curve depends on the fractional void volume. Bulk densities of the order of one-tenth that of solid rock are implied for the upper layers of the surface of the moon.

## INTRODUCTION

The remarkable manner in which the surface of the moon scatters light is well known. *Barabashev* [1922] and *Markov* [1924] discovered that the brightness of almost all areas on the moon peaks sharply at full moon, when the sun is directly behind the observer. This is in contrast to most terrestrial materials, which reflect light more or less in accordance with Lambert's law. *Öpik* [1924] found that the shape of the photometric function is similar for all types of formations. Further, for the same type of formation the maximum of the photometric curve at full moon is independent of position on the lunar disk. These results have been amply confirmed by the measurements of *Bennett* [1938], *Fedoretz* [1952], *van Diggelen* [1959], and others. van Diggelen confirmed Tschunko's assertion that the shape of the scattering law with phase angle is nearly independent of lunar latitude and depends primarily on the lunar longitude. These observations are reviewed by *Minnaert* [1961] and by *Fessenkov* [1962].

Many theoretical attempts have been made to predict this behavior quantitatively. Most of the theoretical models have been based on a smooth surface covered with elevations or depressions of various shapes, such as grooves [*Barabashev,* 1922], spherical domes [*Schönberg,* 1925], or hemiellipsoidal cups [*Bennett,* 1938; *van Diggelen,* 1959]. Such models would appear to be reasonable if the rough, cratered, and cracked topography of the lunar surface on a scale of kilometers is duplicated on a much smaller scale. However, although the formulas based on these models predict the behavior of the lunar photometric function qualitatively, the lack of quantitative agreement is sufficient to cause serious doubts about their applicability to the surface of the moon.

During an experimental study by *Hapke and Van Horn* [1963] of the reflecting properties of surfaces, a number of materials were discovered that scatter light like the moon. All these materials have a porous dendritic or reticulated structure. Thus Hapke was led to consider theoretically reflection from a model surface consisting of a semi-infinite layer of randomly suspended scattering objects.

In this paper the scattering law implicit in such a model is derived. The theoretical law is applied to the lunar surface and compared with the measured photometric curves of the moon. Expressions are found for both the differential brightness of a small region and the integrated brightness of the moon. That there is good agreement between the predicted and measured photometric functions is of particular interest in view of the simplicity of the model.

## DERIVATION

*Assumptions.* The peculiar lunar photometric behavior can be understood as an effect of the shadows cast by obscuring objects arranged in some sort of complex structure. These objects must be large in comparison with a wavelength

of light. If they were comparable with or smaller than a wavelength, they would tend to forward-scatter light as described by the Rayleigh-Gans law, and a sharp backscatter type of reflection would be impossible.

Qualitatively, the backscatter can be explained as follows. When an observer looks parallel to the direction of incident radiation he sees only illuminated surfaces; when he looks in any other direction he sees surfaces partly illuminated and partly in shadow. For this effect to be dominant the albedo of the surface must be small; otherwise, multiple scatterings of the light rays would wash out the shadows, for the brightness of a directly illuminated area is determined by the first power of the albedo whereas the brightness of areas shielded from the source of light depends on second and higher powers of the albedo.

The assumptions of the model surface considered here are as follows.

1. The surface consists of a semi-infinite layer of objects large compared with a wavelength of visible light and arranged in an open network into which light from any direction can penetrate freely. The objects are located irregularly enough within this structure so that on a macroscopic scale the medium appears isotropic and homogeneous.

2. The reflectivity of the individual objects is low, and so only singly scattered light rays are important.

3. The reflecting objects are oriented at random. Thus an effective scattering law for an individual object can be used which is a function only of the angle between the directions of illumination and observation and is otherwise independent of these directions. This assumption is valid for a cloud of particles in suspension, but for a nonsuspension the necessity for support of the reflecting objects will introduce some departure from complete randomness. However, it will be assumed that for the dendritic surface structure under consideration here this departure is so slight that to the approximation of this analysis the assumption is justified.

4. Since the objects that make up the surface are located at random within the array, a typical bundle of light rays penetrating the surface will, owing to absorption and reflection by the objects, experience a gradual attenuation similar to that in a continuous fluid. Thus it will be assumed that the intensity of light is exponentially attenuated in proportion to the path length of the ray through the medium. An important modification to this assumption will be introduced later.

5. All solid angles involved (e.g., those subtended by the light source and detector at the surface and the acceptance cone of the detector) are small.

*Derivation.* The following notation will be used:

$n$ = number of reflecting objects per unit volume.

$d$ = average center-to-center distance between objects; $d = n^{-1/3}$.

$\sigma$ = average cross-sectional area of an object.

$\tau$ = mean attenuation length of a beam of light rays in the medium, i.e. the distance over which the intensity of a beam is attenuated by a factor $e$. If the objects are far apart ($d \gg \sqrt{\sigma}$) it can easily be shown that $\tau = 1/n\sigma$ (cf. *Sears* [1950]). If the objects are close together, shielding of one object by its neighbor will be common so that each object is less efficient at blocking light, and hence $\tau > 1/n\sigma$. However, it will be assumed that to a sufficiently good approximation $\tau = 1/n\sigma$ always.

$b$ = total reflectivity of an object, i.e., the fraction of incident light reflected by the object into all directions. Thus $(1 - b)$ is the fraction absorbed.

$i$ = angle that the direction of incident light makes with the normal to the apparent surface.

$\epsilon$ = angle that a reflected ray reaching the detector makes with the normal to the apparent surface.

$\alpha$ = angle between the directions of incidence and observation.

$d\Omega_\epsilon$ = solid angle subtended at the surface by the detector; $d\Omega_\epsilon \ll 1$.

$a$ = light-sensitive area of the detector.

$R$ = distance of the detector from the apparent surface, measured along the path of a reflected ray. Thus $d\Omega_\epsilon = a/R^2$.

$d\omega$ = solid angle of the acceptance cone of the detector. Light reaching the detector from outside this cone does not register in the detector. $d\omega \ll 1$.

$E_0$ = intensity of incident radiation at the surface, that is, the flux of radiant energy per unit area normal to the direction of incidence.

$\Sigma(\alpha)$ = scattering law of an individual object. Of the light that is reflected, $\Sigma(\alpha)$ is the fraction of light incident from unit solid angle about the direction of incidence that is reflected into unit solid angle about the direction of observation. This quantity is normalized so that

$$\int_{4\pi} \Sigma(\alpha)\, d\Omega = 1$$

The total light reaching the detector is the light scattered from all objects within the detector acceptance cone $d\omega$; this light is then interpreted as having been reflected from the apparent surface area $dA = R^2\, d\omega/\cos\epsilon$. Consider a volume element $dV = r^2 d\omega dr$ located a distance $z$ below the apparent surface and a distance $r$ from the detector (Figure 1). The intensity of light at $dV$ is $E_0 \exp(-z/\tau \cos i)$; and the amount of light reflected from $dV$ toward the detector is $E_0 \exp(-z/\tau \cos i)\, n\sigma dV b\, \Sigma(\alpha)\, a/r^2$.

A naive procedure would then be to assume that this reflected light is further attenuated by an amount $\exp(-z/\tau \cos\epsilon)$ before emerging from the surface, so that the light reaching the detector from $dV$ would be

$$\begin{aligned} dI &= E_0 \exp(-z/\tau \cos i) n\sigma\, dV b \\ &\cdot \Sigma(\alpha) a r^{-2} \exp(-z/\tau \cos\epsilon) \\ &= E_0 n\sigma a b \Sigma(\alpha) r^{-2} \\ &\cdot \exp[-(r-R)\cos\epsilon(\sec i + \sec\epsilon)/\tau] r^2\, d\omega\, dr \\ &= E_0 n\sigma a\, d\omega b \Sigma(\alpha) \\ &\cdot \exp[-(r-R)(1+\cos\epsilon/\cos i)/\tau]\, dr \end{aligned} \quad (1)$$

Indeed, if this assumption is made, and the resulting expression, equation 1, is integrated over all volume elements $dV$ within $d\omega$, the total light $I$ reaching the detector is found to be

$$I = E_0 a\, d\omega b \Sigma(\alpha)/(1 + \cos\epsilon/\cos i) \quad (2)$$

Here $z = (r - R)\cos\epsilon$ and $\tau = 1/n\sigma$ have been used. In equation 2 the factor $(1 + \cos\epsilon/\cos i)^{-1} = \cos i/(\cos i + \cos\epsilon)$ is the well-known Lommel-Seeliger scattering law.

The procedure described in the preceding paragraph neglects an important effect. Even though the objects that form the surface are arranged at random, the direction of incident radiation is still a preferred direction for the reflected light rays. A bundle of light rays entering

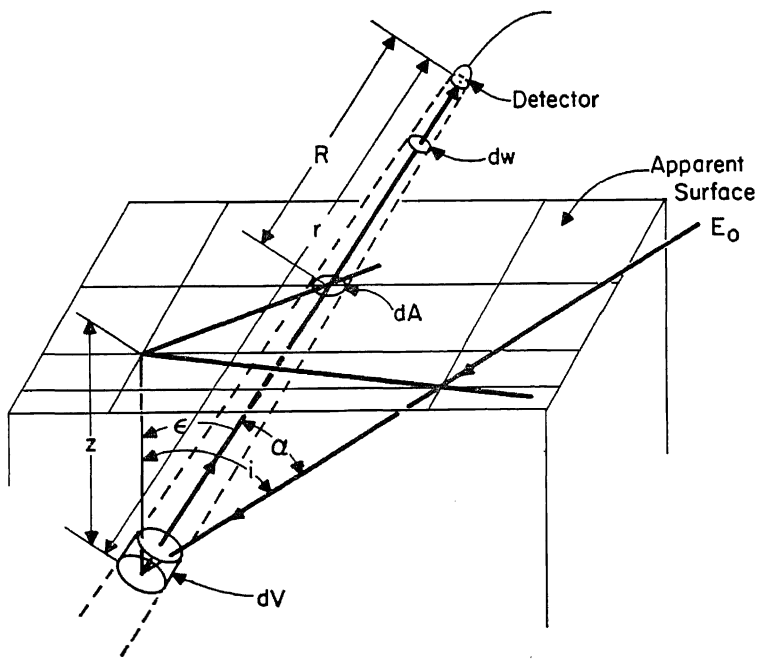


Fig. 1. Geometry of the model surface.

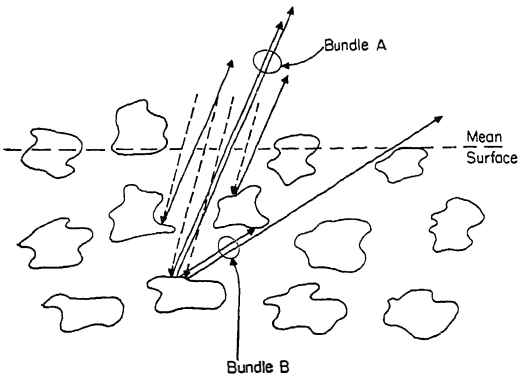


Fig. 2. Actual surface. Bundle of light rays $A$, reflected back toward the direction of incidence, escapes unattenuated, while bundle $B$ is partially blocked.

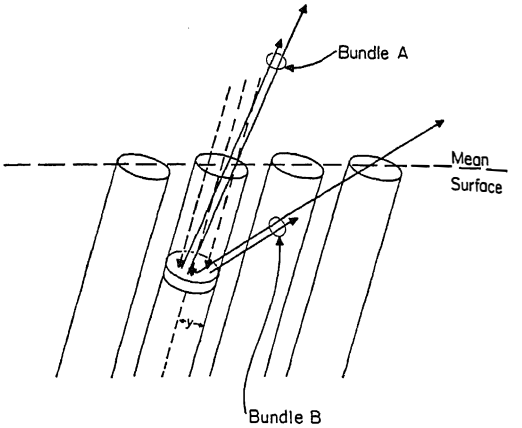


Fig. 3. Idealized model of situation depicted in Figure 2.

the surface will be attenuated on its way in, but the light scattered from deep in the interior of the surface and reflected directly back toward the source can escape unattenuated. That is, if the light is able to penetrate to illuminate an object at a given depth, the light reflected from that object which exactly retraces the path of the incident rays can do so without being blocked. The same will also be true for rays reflected into a small cone about the direction of incidence, the cone of nonattenuation being narrower for rays reflected more deeply under the surface. Bundles of rays scattered into a direction outside this cone will be attenuated through partial blockage by other objects. Figure 2 illustrates this effect.

A simple model that takes account of this effect can be constructed as follows. Instead of considering the idealized surface a homogeneous, absorbing medium, let the surface layer be made up of circular tubes whose radius is of the same order of magnitude as the average spacing between particles and whose axes always remain parallel to the direction of incident radiation. Light entering a cylinder is attenuated exponentially; light rays reflected at a given depth in the cylinder at such an angle as to pass through the wall of the cylinder in which they are reflected are also exponentially attenuated in proportion to their path length, as in Lommel-Seeliger scattering; but reflected rays that do not intersect the wall and that pass out through the end of the tube are not attenuated at all. This model is illustrated in Figure 3.

Let $y$ be the effective radius of these tubes, and let $F(z, \alpha)$ be the fraction of light that is reflected at a given depth $z$ into a direction making an angle $\alpha$ with the direction of incidence and escapes unattenuated from the tube. This fraction $F(z, \alpha)$ is the same as the fractional overlapping area of two circles of radius $y$ whose centers are displaced by amount $z \sec i \tan \alpha$ (see Figure 4), and it is readily found to be

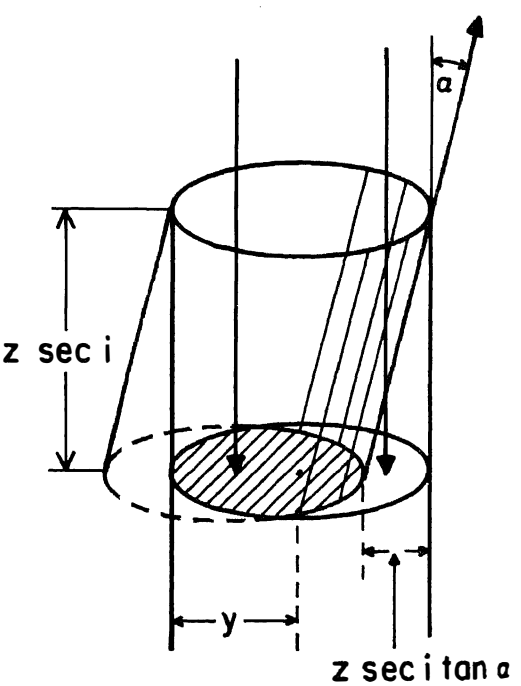


Fig. 4. Reflection from area in tube.

$$F(z, \alpha) = \frac{2}{\pi}\,[\cos^{-1} u - u(1 - u^2)^{1/2}], \quad 0 \le u \le 1$$
$$F(z, \alpha) = 0, \; u < 0, \; u > 1 \qquad (3)$$

where $u = (z \sec i \tan \alpha)/2y$. Thus, in equation 1 the quantity $\exp[-z(\sec i + \sec \epsilon)/\tau]$ must be replaced by

$$F \exp(-z \sec i/\tau) + (1 - F) \exp[-z(\sec i + \sec \epsilon)/\tau] \qquad (4)$$

However, equation 4, as written, violates the reciprocity theorem [*Minnaert*, 1941], which states that the situation in which a ray of light enters a surface from direction $\Omega_i$ and exits into direction $\Omega_\epsilon$ is equivalent to that in which the ray enters from $\Omega_\epsilon$ and exits into $\Omega_i$. This objection can be corrected by noting that the effect $F$ represents will be important only for small values of $\alpha$, at which time $\epsilon$ will be approximately equal to $i$. Thus, to a sufficient degree of accuracy, sec $i$ in the formula for $F$ and also in the first term of (4) can be replaced by sec $i \approx (\sec i + \sec \epsilon)/2$.

With this last change the formula for the amount of light scattered into the detector from $d\omega$ becomes

$$I = E_0 n \sigma a \, d\omega b \Sigma(\alpha) \int_{r=R}^{\infty} \{F(r, \alpha) \cdot \exp[-(r - R)(1 + \cos \epsilon/\cos i)/2\tau] + (1 - F(r, \alpha)) \cdot \exp[-(r - R)(1 + \cos \epsilon/\cos i)/\tau]\} \, dr \qquad (5)$$

where

$$F(r, \alpha) = 2[\cos^{-1} x - x(1 - x^2)^{1/2}]/\pi \quad \text{for} \quad 0 \le x \le 1$$
$$F(r, \alpha) = 0 \quad \text{for} \quad x > 1$$
$$x = (1/4y)(r - R) \cdot (1 + \cos \epsilon/\cos i) \tan \alpha \qquad (6)$$

The integral in equation 5 cannot be evaluated analytically. However, expression 6 for $F$ applies only to tubes of circular cross section, whereas the 'tubes' in the actual surface are of irregular shape, so that the exact expression for $F$ is immaterial. Hence the integration in (5) can be performed by noting that $F$ does not deviate appreciably from the line $(1 - x)$ (in fact, for tubes of square cross section, $F = 1 - x$). Upon putting $F = 1 - x$ for $0 \le x \le 1$, and $F = 0$ for $x > 1$, into (5), the integration is straightforward and gives, after some manipulation,

$$I = E_0 a d\omega b (1 + \cos \epsilon/\cos i)^{-1} \Sigma(\alpha) B(\alpha, g) \qquad (7)$$

where $B(\alpha, g)$ is the retrodirective function

$$B(\alpha, g) = \begin{cases} 2 - \dfrac{\tan \alpha}{2g}(1 - e^{-g/\tan \alpha}) \\ \cdot(3 - e^{-g/\tan \alpha}), \; \alpha \le \pi/2, \\ 1, \; \alpha \ge \pi/2 \end{cases} \qquad (8)$$

and $g = 2y/\tau$.

Equation 7 is the general formula describing the optical reflecting properties of a porous surface sufficiently absorbing so that multiple scattering can be neglected. To apply this equation to the lunar surface the proper individual-particle scattering law must be selected. Depending on the nature of the objects making up the surface this average scattering could be one of three different types: predominantly forward scattering, approximately isotropic scattering, or predominantly backward scattering. Curves representative of the behavior of these different types of reflection laws are plotted in Figure 5. The expressions plotted are:

Forward scattering:

$$\Sigma(\alpha) = \tfrac{4}{9}(1 - \tfrac{1}{2} \cos \alpha)^2$$

Isotropic scattering:

$$\Sigma(\alpha) = 1$$

Backscattering:

$$\Sigma(\alpha) = (\sin \alpha + (\pi - \alpha) \cos \alpha)/\pi$$

Appreciable forward scattering would be expected from transparent, homogeneous spheroids, such as glassy, once-molten droplets of rock. The formula for $\Sigma(\alpha)$ used has no theoretical justification; it was chosen only for its simplicity and because it illustrates forward scattering.

Isotropic scattering might be expected from several different types of particles, such as opaque spheroids with smooth surfaces (e.g., droplets of iron), and irregular translucent par-

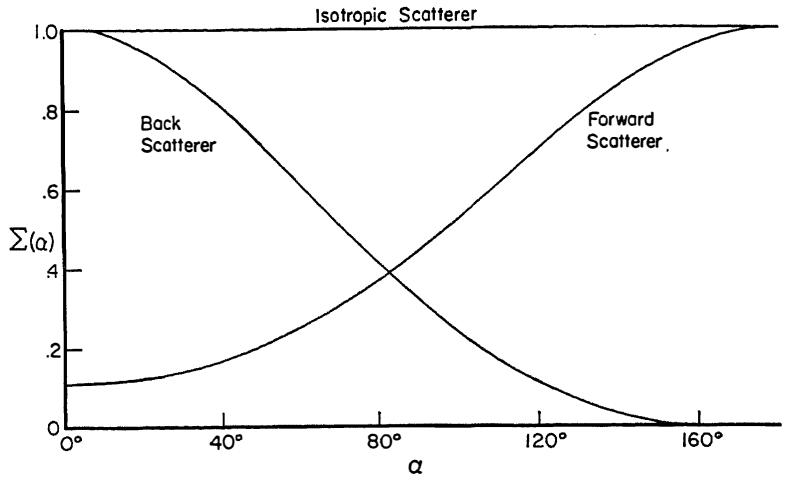


Fig. 5. Typical effective scattering functions of individual particles.

ticles in which most of the scattering is from tiny inhomogeneities within the crystal. An isotropic average scattering law will also result from any group of randomly oriented opaque particles with smooth surface elements that reflect light specularly.

Opaque particles with fairly rough faces oriented at random display an average scattering behavior similar to that of a sphere whose surface elements scatter in accordance with Lambert's law. The scattering function for such a sphere has been worked out by Schönberg [*Van de Hulst*, 1957] and is the third of the functions given above. The broad maximum at $\alpha = 0°$ and minimum at $\alpha = 180°$ is an approximate mathematical description of the fact that the brightest side of a rough, opaque object is the side facing the source of illumination, while the side away from the light is dark.

The result of inserting these three scattering functions for $\Sigma(\alpha)$ into equation 7 is shown in Figure 6 for a surface observed at $\epsilon = 40°$. Only the Schönberg function gives a curve similar to that of the lunar surface. Hence, particles that either are semitransparent or have smooth surfaces are apparently not present in appreciable

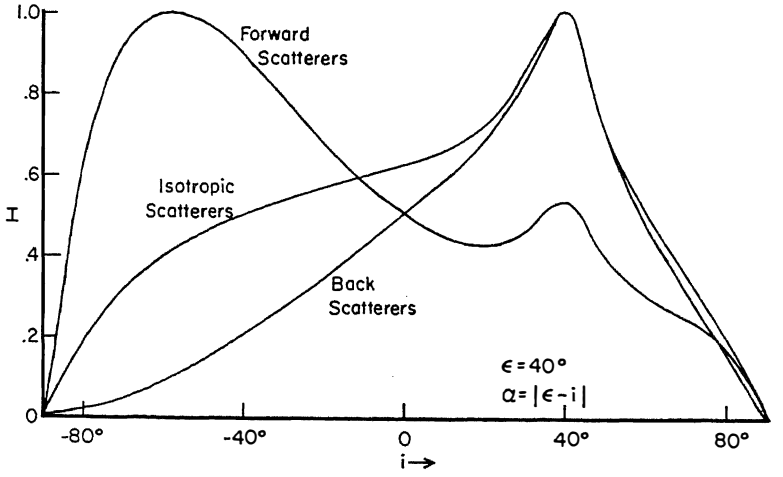


Fig. 6. Photometric functions of surfaces composed of particles which scatter light as shown in Figure 5. The functions illustrated are for a surface oriented 40° from the angle of observation; the directions of observation and illumination remain in the same plane.

quantities on the lunar surface. It may be inferred that the scattering objects are opaque with rough surfaces.

Therefore, we are led to choose a single-particle scattering function of the form

$$\Sigma(\alpha) = (2/3\pi)(\sin\alpha + (\pi - \alpha)\cos\alpha)/\pi \quad (9)$$

where the factor $2/3\pi$ comes from normalizing $\Sigma(\alpha)$. The final form of the scattering law applicable to the lunar surface is thus

$$I(i, \epsilon, \alpha) = E_0 a\, d\omega \frac{2}{3\pi} b \frac{1}{1 + \cos\epsilon/\cos i} \cdot \frac{\sin\alpha + (\pi - \alpha)\cos\alpha}{\pi} B(\alpha, g) \quad (10)$$

where $B(\alpha, g)$ is given by (8). Expression 10 can be converted into the differential scattering law for an element of surface area $dA$ by recalling that $ad\omega = (adA\cos\epsilon)/R^2 = d\Omega_\epsilon dA\cos\epsilon$.

It is of interest to note that expression 10 consists of the product of three functions: the Lommel-Seeliger law, the scattering function for a Schönberg sphere, and the retrodirective function. The retrodirective function gives the sharp backscatter peak at small values of $\alpha$; the Schönberg function determines the shape of the curve at larger phase angles. Since $\Sigma(\alpha)$ is an average reflecting law for randomly oriented particles, sharp variations of $\Sigma(\alpha)$ with $\alpha$ are unlikely; hence the behavior of the scattering function near the peak is relatively insensitive to the exact form of $\Sigma(\alpha)$. The major effect of the Lommel-Seeliger law is to make the scattering function go to zero at $i = \pm 90°$.

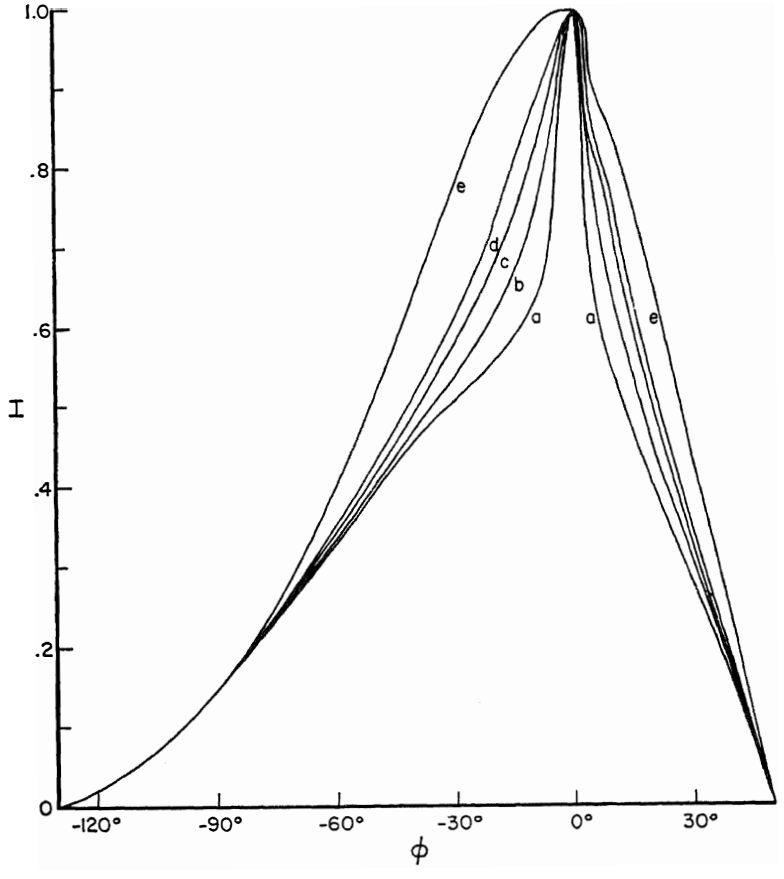


Fig. 7. Photometric functions for a lunar area on the $\lambda = 40°$ meridian, showing the effect of the compaction parameter $g$ on the shape of the curve: $a$, $g = 0.2$; $b$, $g = 0.4$; $c$, $g = 0.6$; $d$, $g = 0.8$; $e$, $g = 2.0$.

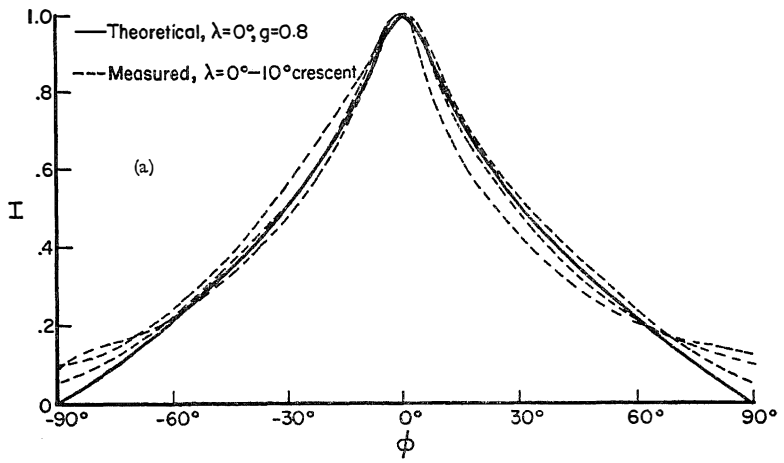
Theoretical, λ=0°, g=0.8
Measured, λ=0°–10° crescent
(a)
I
1.0
.8
.6
.4
.2
0
-90°
-60°
-30°
0°
30°
60°
90°
ϕ

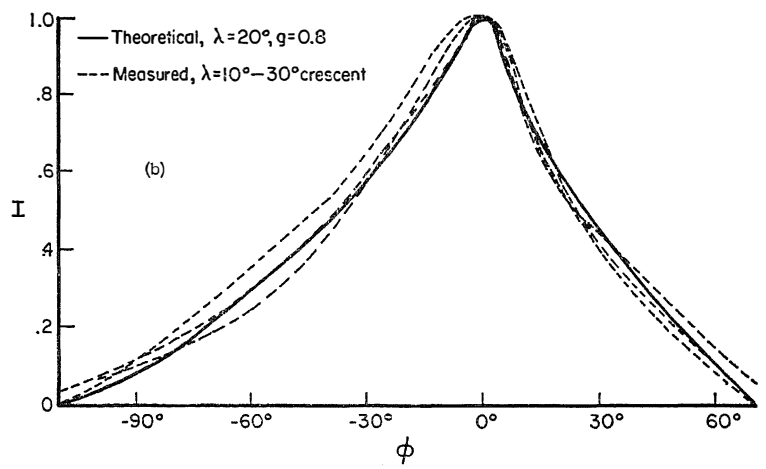
Theoretical, λ=20°, g=0.8
Measured, λ=10°–30° crescent
(b)
I
1.0
.8
.6
.4
.2
0
-90°
-60°
-30°
0°
30°
60°
ϕ

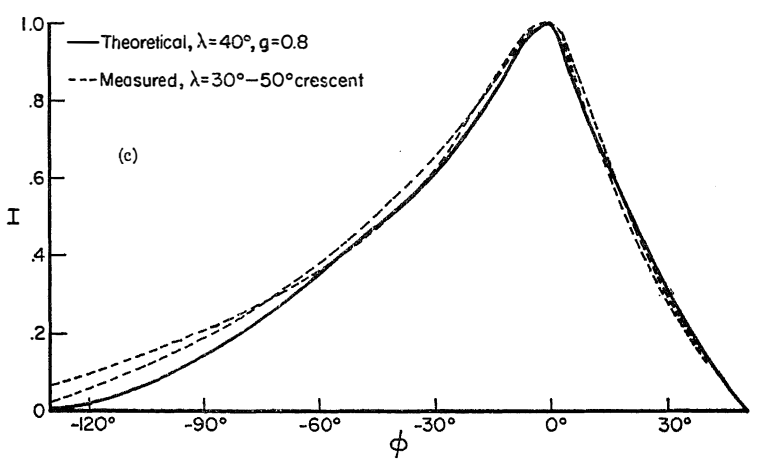
Theoretical, λ=40°, g=0.8
Measured, λ=30°–50° crescent
(c)
I
1.0
.8
.6
.4
.2
0
-120°
-90°
-60°
-30°
0°
30°
ϕ

Fig. 8

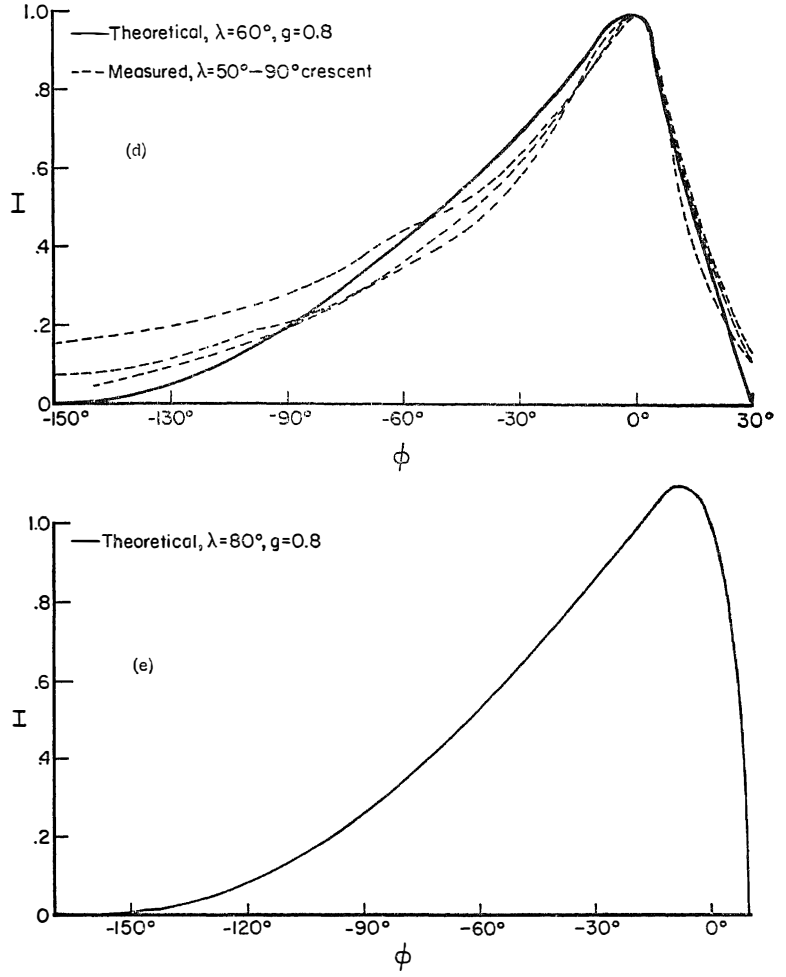


Fig. 8. Plots of the theoretical photometric function compared with average measured lunation curves for various crater floors. Solid line: equation 11 with $E_0 a d\omega 2b/3\pi = 1$ and $g = 0.8$. Dashed curves: average lunation curves (after *van Diggelen* [1959], Figure 73).

## Applications to the Moon

*Differential scattering law.* In applying expression 10 to the moon as observed from the earth it is sufficiently accurate to assume that the intensity equator coincides with the geographic equator and that the subearth point falls on this line at the center of the lunar coordinate system. (For more exact comparisons equation 10 should be used.) Then it can easily be shown that

$$\cos \epsilon = \cos \beta \cos \lambda$$

$$\cos i = \cos \beta \cos (\lambda + \phi)$$

$$\alpha = |\phi|$$

where $\beta$ is the lunar latitude of the area of interest, $\lambda$ is its longitude, and $\phi$ is the lunar phase angle.

Making these substitutions in equation 10 it is found that the amount of light reflected into a terrestrial detector from a small portion of the surface at position $(\lambda, \beta)$ on the moon at phase angle $\phi$ is

$$I(\phi, \lambda, \beta) = E_0 a \, d\omega \frac{2}{3\pi} b \frac{1}{1 + \cos \lambda / \cos (\lambda + \phi)} \cdot \frac{\sin |\phi| + (\pi - |\phi|) \cos |\phi|}{\pi} B(\phi, g) \quad (11)$$

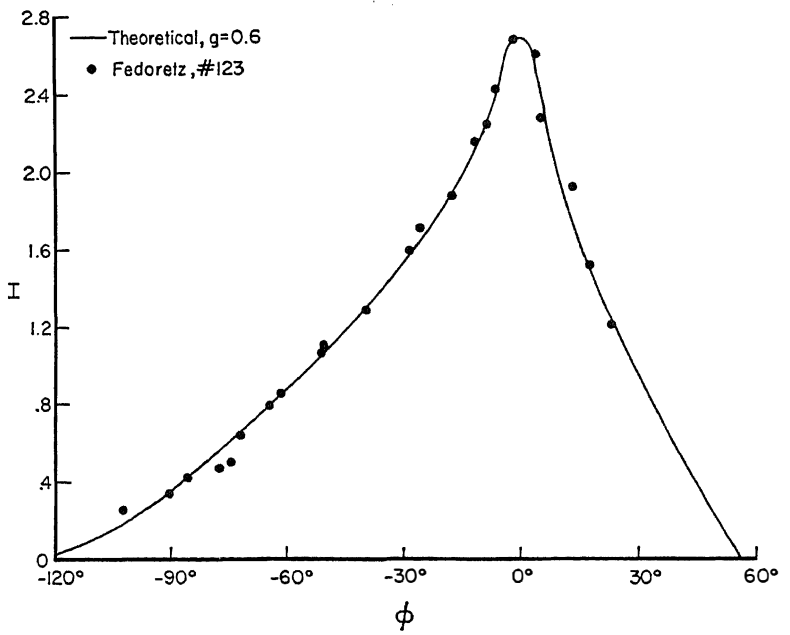


Fig. 9. Mountain region below Mare Nectaris.

where

$$B(\phi, g) = \begin{cases} 2 - \dfrac{\tan|\phi|}{2g}\left(1 - e^{-g/\tan|\phi|}\right) \\ \cdot\left(3 - e^{-g/\tan|\phi|}\right), \ |\phi| \leq \pi/2, \\ 1, \ |\phi| \geq \pi/2 \end{cases}$$

Normalized curves of equation 11 are plotted in Figure 7 for an area on the $\lambda = +40°$ meridian. In that figure the effect of varying the parameter $g$ on the width of the peak is shown. Comparisons of the scattering formula with the measured brightness of various areas on the moon are given in Figures 8 to 15. In Figure 8 the normalized theoretical curve with $g = 0.8$ is compared with *van Diggelen's* [1959] average normalized curves of crater floors. In Figures 9 to 15 the theoretical curve is plotted along with measured points of *Fedoretz* [1952] for specific lunar areas selected more or less at random. For these figures the compaction parameter $g$ has been chosen to give the best fit;

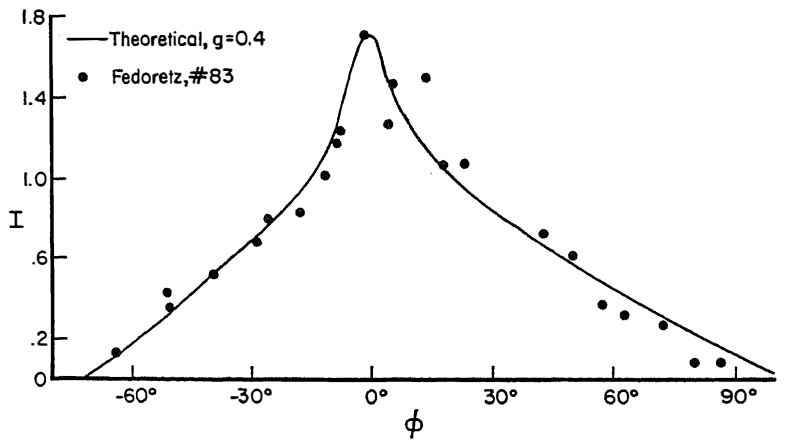


Fig. 10. Mare Imbrium.

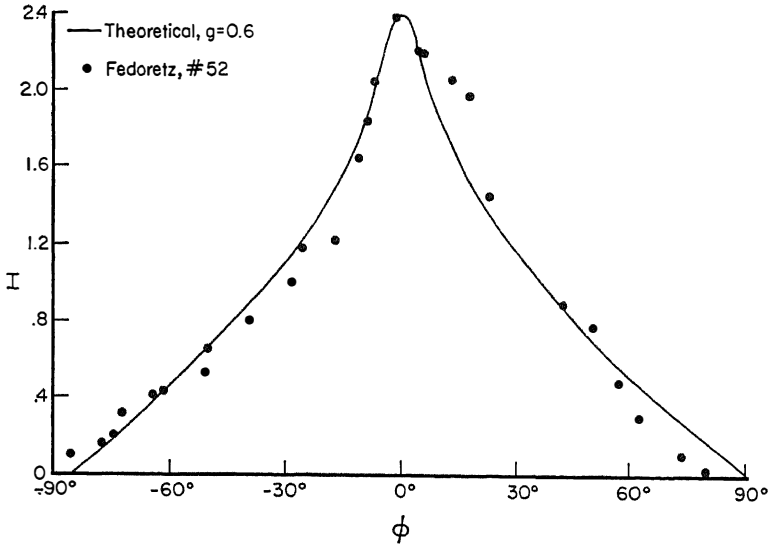


Fig. 11. Ptolemaeus (center).

and $(E_0 a d\omega 2b/3\pi)$ has been set numerically equal to Fedoretz's ordinate at the peak of the curve. Since $b$ and $g$ are related to the composition and structure of an individual area, variations of these parameters from place to place on the moon are to be expected.

Several important features of the photometric function represented by equation 11 should be noted.

1. The differential intensity rises to a sharp maximum at or very close to full moon ($\phi = 0$) for all areas on the lunar disk.

2. The amount of light reflected from a small region toward the detector at full moon is $E_0 a d\omega (2/3\pi) b$, which is constant for all materials of the same composition (same value of $b$), independent of location on the lunar disk.

3. The photometric function is independent of lunar latitude $\beta$, in agreement with the observations of Tschunko and of van Diggelen.

4. Normal albedo: The normal albedo of a surface is defined [*Minnaert,* 1961] to be the ratio of the brightness of the surface to that of a perfectly reflecting Lambert surface, both sur-

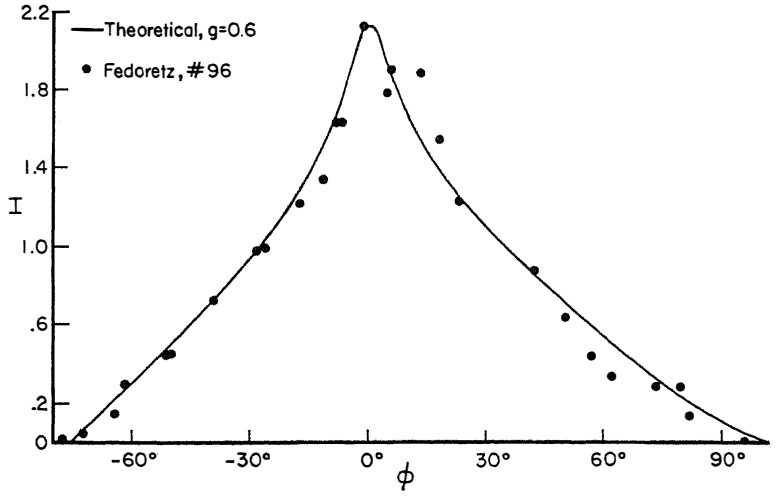


Fig. 12. Pitatus.

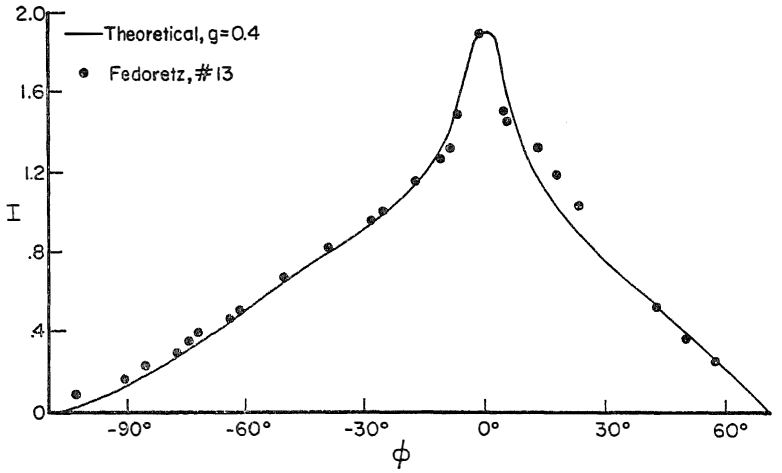


Fig. 13. Bright ray in Mare Serenitatis.

faces being illuminated and observed normally. Since a perfect Lambert surface has the reflection law $I_L = E_0 a d\omega\ (1/\pi)\cos i$, the normal albedo $a_n$ is seen to be

$$a_n = I(\phi = 0)/I_L(i = 0) = 2b/3 \qquad (12)$$

Values of $a_n$ on the lunar surface range from about 6 to 18 per cent; thus the reflectance $b$ of the individual particles varies between 9 and 27 per cent.

5. The sharpness of the peak at full moon is determined by the parameter $g = 2y/\tau$. Most of the lunar surface appears to be fitted most closely by curves with $g = 0.6$, although areas with $g$ from 0.4 to 0.8 are encountered, the smaller values of $g$ being associated more often with the rays and the larger values with dark crater floors.

This parameter is closely related to the degree of compaction of the surface, as can be seen by recalling that $\tau = 1/n\sigma = d^3/\sigma$. Thus, $g = 2(y/d)(\sigma/d^2)$. Let $\rho/\rho_0$ be the relative density of the surface, i.e. the fractional volume of the surface occupied by solid matter. Then it is evident that $\rho/\rho_0 = (\sigma/d^2)^{3/2}$. Also, $y$ is a distance of order $d$. Hence

$$g = k(\rho/\rho_0)^{2/3} \qquad (13)$$

where $k$ is a dimensionless number approximately equal to 2. Thus the upper portions of the lunar surface are seen to be in an extremely low state of compaction with relative densities of the order of 15 per cent or less. This deduction is in full agreement with radio-frequency and infrared observations (summarized by *Sin-*

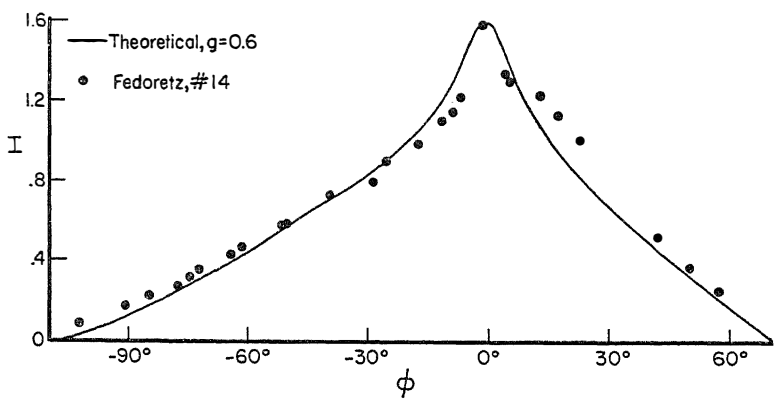


Fig. 14. Area next to ray in Serenitatis.

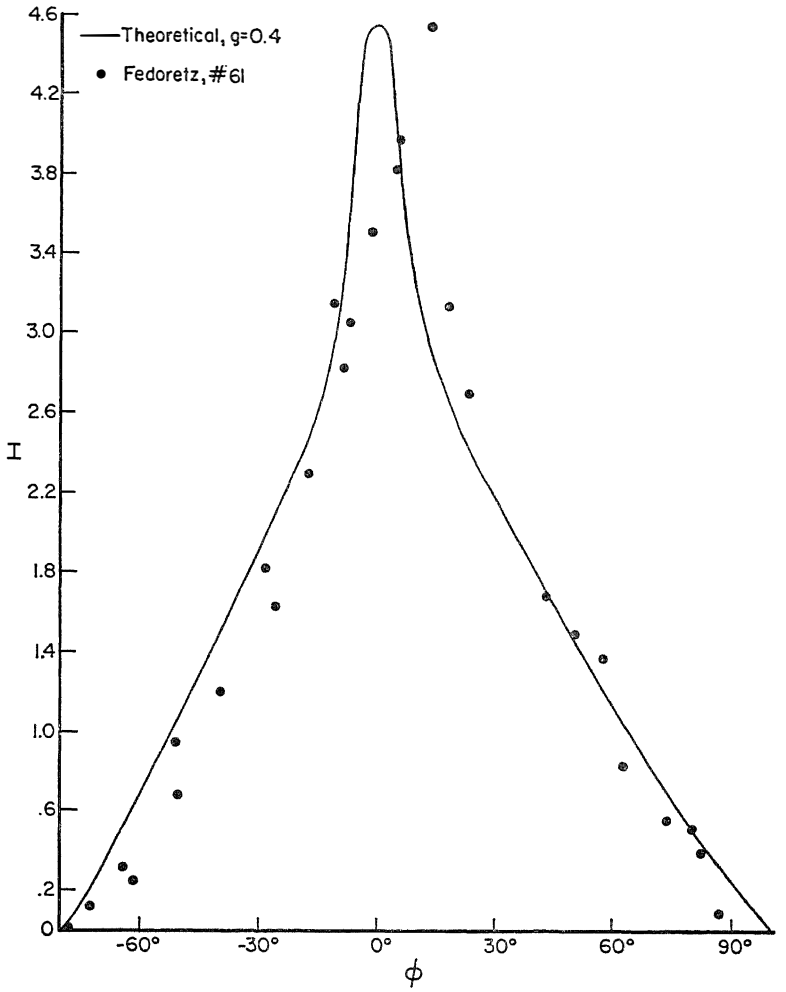


Fig. 15. Tycho floor.

*ton* [1962]), which imply that the thermal inertia and thus the density of the lunar surface are extremely low. It is also in agreement with laboratory measurements [*Hapke and Van Horn*, 1963]: all the different types of surfaces that have been found experimentally to scatter light in the same manner as the lunar surface have had relative densities of the order of 10 per cent.

Upper and lower bounds on $g$ are required by physical considerations. Since the relative density cannot exceed unity, $g$ must be less than about 2 for the model to be applicable. The lower limit is set by diffraction. The particles must cast sharp shadows, which cannot occur if there is appreciable diffraction around the edges of the particles. Thus the condition $\sigma^{1/2}/\tau \gtrsim (\lambda/\pi\tau)^{1/2}$ is necessary, which requires $g = 2(y/d)(\sigma/d^2) \gtrsim 2(y/d)(\lambda/\pi d)^{1/2} \approx (\lambda/d)^{1/2}$. For $d = 1$ cm, $g \gtrsim 0.01$; for $d = 10$ microns, $g \gtrsim 0.2$.

6. The lunar rays exhibit the same type of reflection properties as the rest of the surface, but somewhat enhanced. According to the model presented here no special hypothesis need be invoked to explain the rays. They are merely an optically thick layer of material of slightly higher average reflectance and in a somewhat lower state of compaction than the territory on which they lie.

*Integrated photometric law.* Upon integrating equation 11 over the part of the lunar sphere that is both visible and illuminated, the follow-

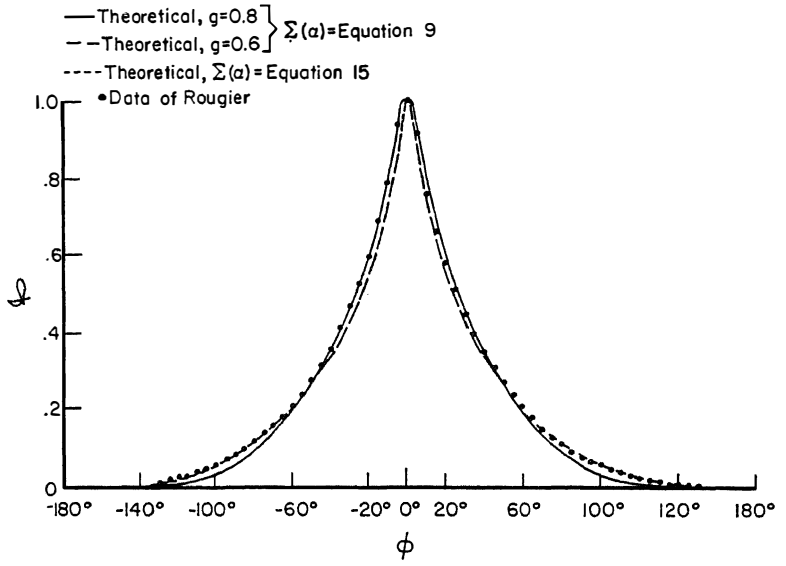


Fig. 16. Integrated brightness of moon.

ing expression for the integrated brightness of the moon during a lunation is obtained:

$$\mathcal{J} = E_0 \pi R_m^2 \, d\Omega_\epsilon \frac{2}{3\pi} b \cdot \frac{1}{2}\left[1 - \sin\frac{|\phi|}{2}\tan\frac{|\phi|}{2}\ln\left(\cot\frac{|\phi|}{4}\right)\right] \cdot \frac{\sin|\phi| + (\pi - |\phi|)\cos|\phi|}{\pi} B(\phi, g) \quad (14)$$

where $R_m$ is the radius of the moon, and $\mathcal{J}$ is the total amount of light incident on the detector.

Equation 14 is plotted in Figure 16 along with Rougier's measurements on the integrated light from the moon [*van Diggelen*, 1959]. Note that the curve for $g = 0.8$ best fits the data for negative phase angles, whereas $g = 0.6$ provides a better fit for positive phases. The measured curve will, of course, be influenced by differences in large individual areas on the moon, so that such an effect is not surprising. It implies that the western (astronomical) hemisphere has a slightly larger average compaction than the eastern hemisphere. That is, the lighter-colored highlands, which are in greater abundance in the western hemisphere, apparently tend to be somewhat more compact than the darker maria, which predominate in the eastern hemisphere.

Taking the magnitude of the full moon relative to the sun as $m = 14.04$, a straightforward calculation gives the average reflectance of the particles making up the lunar surface as $b = 0.18$, and hence the average normal albedo of the lunar surface is $a_n = 0.12$.

The theoretical integrated light curve falls slightly below the measured data at larger phase angles. This departure may be strictly fortuitous, since brighter upland areas seem to be more plentiful in the limb regions than darker maria. It might also be possible to account for it by secondary scattering.

The effect of secondary scattering on the photometric curves may be estimated as follows. For the Schönberg scattering function more than 80 per cent of the light incident on a particle is scattered back within 30° of the direction of incidence. Hence, in the first approximation the singly reflected rays can be treated as a weak second source of radiation located under the surface and shining directly back toward the sun. Including this effect in the model is quite straightforward and results only in replacing the effective individual-particle scattering law by

$$\Sigma(\alpha) = (2/3\pi)[(\sin\alpha + (\pi - \alpha)\cos\alpha)/\pi + b(\sin\alpha - \alpha\cos\alpha)/2\pi]$$

This correction is quite minor and can be shown to be insufficient to account for the excess brightness at large phase angles. Since the

direction of a ray in the surface becomes randomized only when the ray is reflected more than twice, the shape of the photometric function will be affected by multiple scattering only when the condition $b^2 \ll 1$ is no longer satisfied. This explains how $b$ can be as large as 30 per cent on the moon and still a sharp backscatter peak can be observed.

The minor discrepancy between the theoretical and measured intensities at large phase angles can be fully accounted for by introducing a small amount of forward scattering into $\Sigma(\alpha)$. *Richter* [1962] has measured the average scattering properties of particles of various size ranges. He finds that rough particles, large in comparison with a wavelength, have in addition to the main backscatter peak a narrow, high, forward-scatter peak which arises from diffraction of light around small irregularities on the limbs of the particles. A more accurate photometric formula should include this effect in the expression for $\Sigma(\alpha)$. A good fit to Rougier's data can be obtained by using

$$\Sigma(\alpha) = (2/3\pi)[(\sin\alpha + (\pi - \alpha)\cos\alpha)/\pi + 0.1(1 - \cos\alpha)^2] \quad (15)$$

Other differences between the theoretical and measured photometric functions should be discussed. The theoretical function predicts that, contrary to observations, the brightness of areas close to the limb do not peak at exactly full moon. For longitudes $\lambda$ less than a critical value $\lambda_c$, given by $\tan\lambda_c = 1.5/g$, equation 11 peaks at $\phi = 0$, while for $|\lambda| > \lambda_c$ the peak is shifted slightly toward local noon and is increased somewhat over the full-moon value (see Figure 8*e*). For $g = 0.6$, $\lambda_c = 68°$. This limb anomaly arises from the simplifying assumption that the change in average density at the apparent surface is a step function, whereas the actual density distribution increases gradually over a distance of the order of several times $d$.

A small but peculiar departure from the photometric behavior of most of the lunar surface is displayed by a number of bright rayed craters, such as Tycho, Aristarchus, and Proclus. The peaks of the photometric curves of these areas are as sharp as those of the rest of the moon, but the maximum brightness occurs slightly *after* full moon, independently of whether the crater is on the eastern or the western hemisphere (Figure 15). This behavior (if real) is extremely puzzling; it implies a preferred alignment of the surface particles and cannot be explained by any simple assumptions, such as fluorescence or different orientation of the mean surface. One way of obtaining such a shift in the phase angle of the maximum while retaining the sharpness would be to mix flat, smooth flakes, whose surfaces reflect light specularly, with the rough, irregular objects comprising most of the lunar surface, the flakes having their faces preferentially oriented toward the east. How such alignment could arise or be maintained is unknown.

## Conclusions

An expression that describes the scattering of light from a dark, intricate surface has been derived theoretically. The success of the model in duplicating the measured lunar photometric data allows several important properties of the microstructure of the lunar surface to be inferred.

Whatever the nature or history of the lunar materials, the surface layer is porous, with many interconnecting cavities into which light from any direction can penetrate freely. Voids occupy of the order of 90 per cent of the total volume of the layer. The objects composing the surface are larger than a wavelength of light, absorb 70 per cent or more of the light incident on them, and are opaque, with fairly rough surfaces. Few objects that either are semitransparent or have smooth surfaces can be present. Differences in brightness of various areas on the moon are caused by variations, which arise from differences of chemical composition and of times of exposure to the darkening effect of solar corpuscular radiation, in the absorbing properties of the objects. The rays whose photometric curves exhibit the sharpest peaks at full moon have surface layers with the lowest compactions.

These requirements exclude a surface of bare rock perforated by cracks or craters and also layers of volcanic foam or scoriaceous rock, since in such materials the cavities are isolated. However, from laboratory experiments [*Hapke and Van Horn*, 1963] it is known that finely divided dielectric powders can build a dendritic surface with the required topography. Thus the peculiar photometric properties of the moon can be fully accounted for by a layer of darkened, pulverized rock dust covering the lunar surface.

*Acknowledgments.* It is a pleasure to acknowledge the discussions with T. Gold, H. Van Horn, and M. Harwit of the Cornell University Center for Radiophysics and Space Research, which contributed greatly to my understanding of this subject. I especially wish to thank Mrs. L. Pollock for computing and plotting the curves that appear in this paper.

This research is sponsored by the National Aeronautics and Space Administration under grant NsG-119-61.

## References

Barabashev, N. P., Bestimmung der Erdalbedo und des Reflexionsgesetzes für die Oberflache der Mondmeere Theorie der Rillen, *Astron. Nachr., 217,* 445–452, 1922.

Bennett, A. L., A photovisual investigation of the brightness of 59 areas on the moon, *Astrophys. J., 88,* 1–26, 1938.

Fedoretz, V. A., Photographic photometry of the lunar surface, *Publ. Kharkov Obs., 2,* 49–172, 1952.

Fessenkov, V. G., Photometry of the moon, in *Physics and Astronomy of the Moon,* edited by Z. Kopal, pp. 99–128, Academic Press, New York, 1962.

Hapke, B., and H. Van Horn, Photometric studies of complex surfaces, with applications to the moon, *J. Geophys. Res., 68*(15), 1963.

Markov, A., Les particularités dans la réflexion de la lumière par la surface de la lune, *Astron. Nachr., 221,* 65–78, 1924.

Minnaert, M., The reciprocity principle in lunar photometry, *Astrophys. J., 93,* 403–410, 1941.

Minnaert, M., Photometry of the moon, in *Planets and Satellites, The Solar System,* edited by G. P. Kuiper and B. M. Middlehurst, vol. 3, pp. 213–245, University of Chicago Press, 1961.

Öpik, E., Photometric measures on the moon and the earth-shine, *Publ. Astron. Obs. Tartu, 26,* 1–68, 1924.

Richter, N. B., The photometric properties of interplanetary matter, *Quart. J. Roy. Astron. Soc., 3,* 179–186, 1962.

Schönberg, E., Untersuchungen zur Theorie der Beleuchtung des Mondes auf Grund photometrischer Messungen, *Acta Soc. Sci. Fennicae, 50,* 1–70, 1925.

Sears, F. W., *Introduction to Thermodynamics, Kinetic Theory of Gases, and Statistical Mechanics,* chapter 13, Addison-Wesley Publishing Company, Cambridge, Mass., 1950.

Sinton, W., Temperatures on the lunar surface, in *Physics and Astronomy of the Moon,* edited by Z. Kopal, pp. 407–427, Academic Press, New York, 1962.

Van de Hulst, H. C., *Light Scattering by Small Particles,* John Wiley & Sons, New York, 1957.

van Diggelen, J., Photometric properties of lunar crater floors, *Rech. Obs. Utrecht, 14,* 1–114, 1959

(Manuscript received March 13, 1963;
revised May 21, 1963.)